



University of Dundee

## Cytochrome P450 Epoxygenase-Derived Epoxyeicosatrienoic Acids Contribute to Insulin Sensitivity in Mice and in Humans

Gangadhariah, Mahesha. H. ; Dieckmann, Blake W.; Lantier, Louise; Kang, Li; Wasserman, David H.; Chiusa, Manuel; Caskey, Charles F.; Dickerson, Jaime; Luo, Pengcheng; Capdevila, Jorge H.; Imig, John D.; Yu, Chang; Pozzi, Ambra; Luther, James M.

*Published in:*  
Diabetologia

*DOI:*  
[10.1007/s00125-017-4260-0](https://doi.org/10.1007/s00125-017-4260-0)

*Publication date:*  
2017

*Document Version*  
Peer reviewed version

[Link to publication in Discovery Research Portal](#)

*Citation for published version (APA):*

Gangadhariah, M. H., Dieckmann, B. W., Lantier, L., Kang, L., Wasserman, D. H., Chiusa, M., ... Luther, J. M. (2017). Cytochrome P450 Epoxygenase-Derived Epoxyeicosatrienoic Acids Contribute to Insulin Sensitivity in Mice and in Humans. *Diabetologia*, 60(6), 1066-1075. <https://doi.org/10.1007/s00125-017-4260-0>

### General rights

Copyright and moral rights for the publications made accessible in Discovery Research Portal are retained by the authors and/or other copyright owners and it is a condition of accessing publications that users recognise and abide by the legal requirements associated with these rights.

- Users may download and print one copy of any publication from Discovery Research Portal for the purpose of private study or research.
- You may not further distribute the material or use it for any profit-making activity or commercial gain.
- You may freely distribute the URL identifying the publication in the public portal.

# **Cytochrome P450 Epoxygenase-Derived Epoxyeicosatrienoic Acids Contribute to Insulin Sensitivity in Mice and in Humans**

M.H. Gangadhariah<sup>1</sup>, B.W. Dieckmann<sup>1</sup>, L. Lantier<sup>2</sup>, L. Kang<sup>2</sup>, D.H. Wasserman<sup>2</sup>, M. Chiusa<sup>1</sup>,  
C.F. Caskey<sup>3</sup>, J. Dickerson<sup>4</sup>, P. Luo<sup>5</sup>, J.H. Capdevila<sup>1</sup>, J.D. Imig<sup>6</sup>, C. Yu<sup>7</sup>, A. Pozzi<sup>1,9</sup>, J.M.  
Luther<sup>1,8</sup>

## **Running title: CYP2C-derived EETs and Insulin sensitivity**

1. Division of Nephrology and Hypertension, Department of Medicine, Vanderbilt University School of Medicine, Nashville, TN
2. Department of Molecular Physiology and Biophysics, Vanderbilt University School of Medicine, Nashville, TN
3. Department of Radiologic Sciences, Vanderbilt University School of Medicine, Nashville, TN
4. Florida Atlantic University Charles E. Schmidt College of Medicine, Boca Raton, FL
5. Huangshi Central Hospital, Hubei Province, People's Republic of China
6. Department of Pharmacology and Toxicology, Cardiovascular Research Center, Medical College of Wisconsin, Milwaukee, Wisconsin
7. Department of Biostatistics, Vanderbilt University School of Medicine, Nashville, TN
8. Division of Clinical Pharmacology, Department of Medicine, Vanderbilt University School of Medicine, Nashville, TN
9. Department of Veteran Affairs, Nashville, TN

### **Corresponding Authors**

James M. Luther, MD MSCI and Ambra Pozzi, PhD  
2200 Pierce Ave.  
560 RRB  
Vanderbilt University Medical Center  
Nashville, TN 37232-6602  
Phone: (615) 936-3420  
Fax: (615) 936-2746  
E-mail: [James.Luther@Vanderbilt.edu](mailto:James.Luther@Vanderbilt.edu)  
Email: [Ambra.Pozzi@Vanderbilt.edu](mailto:Ambra.Pozzi@Vanderbilt.edu)

**Abstract word count:** 246

**Main text word count:** 3529

**Legend text:** 460

**Total Text:** 3989

**Figures:** 6

**Tables:** 2

**References:** 49

## ABSTRACT

*Aims/hypothesis:* Insulin resistance is frequently associated with hypertension and type 2 diabetes. The P450 arachidonic acid epoxygenases (CYP2C, CYP2J) and their epoxyeicosatrienoic acid (EET) products lower blood pressure and may also improve glucose homeostasis. However, the direct contribution of endogenous EET production on insulin sensitivity has not been previously investigated. In this study we tested the hypothesis that endogenous CYP2C-derived EETs alter insulin sensitivity by analyzing mice lacking *Cyp2c44*, a major EET producing enzyme, and by testing the association of plasma EETs with insulin sensitivity in humans.

*Methods:* We assessed insulin sensitivity in wild-type (WT) and *Cyp2c44(-/-)* mice using hyperinsulinaemic-euglycaemic clamps and isolated skeletal muscles. Insulin secretory function was assessed using hyperglycaemic clamps and isolated islets. Vascular function was tested in isolated-perfused mesenteric vessels. Insulin sensitivity and secretion were assessed in humans using frequently sampled intravenous glucose tolerance tests and plasma EETs were measured by mass spectrometry.

*Results:* *Cyp2c44(-/-)* mice showed decreased insulin sensitivity compared to WT controls. Although glucose uptake was diminished in *Cyp2c44(-/-)* mice *in vivo*, insulin-stimulated glucose uptake was unchanged *ex vivo* in isolated skeletal muscle. Capillary density was similar but vascular  $K_{ATP}$ -induced relaxation was impaired in isolated *Cyp2c44(-/-)* vessels, suggesting that impaired vascular reactivity produces impaired insulin sensitivity *in vivo*. Similarly, plasma EETs positively correlated with insulin sensitivity in human subjects.

*Conclusions/Interpretation:* CYP2C-derived EETs contribute to insulin sensitivity in mice and in humans. Interventions to increase circulating EETs in humans could provide a novel approach to improve insulin sensitivity and treat hypertension.

**Key Words:** Arachidonic Acid, Insulin Sensitivity, Insulin Secretion *in vitro* and *in vivo*, Hypertension, epoxygenases

## INTRODUCTION

Obesity, hypertension, and type 2 diabetes (T2DM) are linked by insulin resistance and endothelial dysfunction, although the causative etiology of these associations remains unclear. Compensatory hyperinsulinaemia in insulin-resistant subjects has been associated with cardiovascular events and has been implicated in the development of hypertension [1, 2]. The P450 arachidonic acid epoxygenases (CYP2C, CYP2J) and their epoxyeicosatrienoic acid (EET) products lower blood pressure via renal and vascular effects [3] and may also improve glucose homeostasis.

The CYP arachidonic acid (AA) monooxygenases oxidize AA to 5,6-, 8,9-, 11,12-, or 14,15-EET via CYP2 isoforms or to 19- or 20-hydroxyeicosatetraenoic acid (HETE) via CYP4 isoforms. EETs are hydrolyzed to less biologically active dihydroxyeicosatrienoic acids (DHETs) by soluble epoxide hydrolase (sEH) [3-6]. EETs act as endothelium-derived vasodilators [7] and in mice, multiple isoforms possess EET synthase activity (e.g., Cyp2c40 and Cyp2c44). Cyp2c44 is expressed in the vascular endothelium, kidney, and liver, and Cyp2c44 disruption alters sodium handling and causes hypertension in response to dietary sodium or potassium loading [8-10]. Hepatic and vascular CYP2C expression and activity are decreased in rodent models of insulin resistance [11, 12]. Furthermore, decreasing EET hydrolysis by sEH inhibition or deleting the gene encoding sEH results in increased insulin sensitivity and insulin secretion in rodents [13-15]. This effect of sEH inhibitors on insulin sensitivity is likely mediated via EETs, although the effect of disrupting endogenous EET production on insulin sensitivity has not been previously investigated.

Although insulin resistance is associated with increased cardiovascular events [16], therapies which improve insulin sensitivity (e.g., thiazolidinediones) have not improved cardiovascular

outcomes [17]. Therefore, novel therapeutic targets are needed which improve both insulin sensitivity and hypertension control. EET agonists reduce blood pressure and improve glucose metabolism [11, 18]. In this study, we investigated the effect of endogenous EETs on peripheral and hepatic insulin sensitivity in mice lacking Cyp2c44 expression, and examine the association between plasma EETs and insulin sensitivity in humans.

## METHODS

*Animals.* All experiments were approved by the Vanderbilt and Medical College of Wisconsin Institutional Animal Care and Use Committees, and NIH principals of laboratory animal care were followed. Six week-old 129SvJ male mice were randomized to either a normal chow or high fat (HF) diet (with 60% fat by calorie content, BioServ, Frenchtown, NJ) for 12 weeks with free access to water and housed in a temperature-controlled facility with a 12-hour light/dark cycle.

*Hyperinsulinaemic-euglycaemic and hyperglycaemic clamps.* Body composition was measured (MiniSpec LF50, Bruker Optics Ltd., The Woodlands, TX). Carotid arterial and jugular venous catheters were implanted  $\geq 3$  days prior to study, and clamps were conducted in the Vanderbilt Mouse Metabolic Center (<https://labnodes.vanderbilt.edu/mmpc>) [19]. The glucose infusion rate (GIR) was varied to maintain whole blood glucose at  $\sim 115$  mg/dL (6.4 mmol/L) during euglycaemic clamps and  $\sim 250$  mg/dL (13.9 mmol/L) during hyperglycaemic clamps (ACCU-CHEK, Roche Diagnostics, Basel, Switzerland). Endogenous glucose appearance ( $\text{EndoR}_a$ ) was determined by  $[3\text{-}^3\text{H}]\text{-glucose}$  tracer and tissue specific glucose uptake by  $^{14}\text{C}\text{-2-deoxyglucose}$  tracer (2-DG; Perkin Elmer, Waltham, MA) as described previously [19]. Insulin ( $4\text{ mU}\cdot\text{kg}^{-1}\cdot\text{min}^{-1}$ ; Novo-Nordisk, Princeton, NJ) was infused, and after the last sample, mice were euthanized and tissues were collected and stored at  $-80\text{ }^\circ\text{C}$ . Plasma insulin was measured by radioimmunoassay [19].

*Islet isolation and static incubation.* Pancreatic islets were isolated from male WT and *Cyp2c44(-/-)* at 12-16 weeks of age as previously described [19]. Islets were matched for size and number, and assessed as islet equivalents (IEQ). After isolation, glucose-stimulated insulin

secretion was assessed in parallel for 60 minutes at 37 °C in 2 mL fresh RPMI-1640 containing either 5.5 or 16.7 mmol/L glucose.

*Glucose tolerance tests and glyburide-stimulated insulin secretion.* Studies were performed according to the National Mouse Metabolic Phenotyping Centers glucose tolerance test [<https://www.mmpc.org/shared/protocols.aspx>]. Mice were fasted for 5-hours starting at 7AM. During glucose tolerance tests, 20% dextrose (2g/kg) was administered i.p., and tail-vein blood glucose was measured. During glyburide tests, glyburide (1.25mg/kg i.p.; 0.083mg/mL in sterile saline + 0.2% DMSO; Merck Millipore, Darmstadt, Germany) was administered and saphenous vein blood was collected before and at 15 minutes for insulin assay [20, 21].

*Western blots.* Homogenized skeletal muscle or liver protein samples were separated by 12% SDS-PAGE and membranes were then incubated with anti- Kir6.1 (1:200 dilution; Alomone Labs, Jerusalem, Israel), anti-Kir6.2 (1:1000 dilution; Alomone Labs), anti- $\beta$ -tubulin (1:2000 dilution; Cell Signaling Technology; MA, USA), anti-pAKT (1:1000, Cell Signaling Technology), or anti-AKT (1:1000, Cell Signaling Technology) antibodies followed by horseradish peroxidase conjugated secondary antibody (Cell Signaling Technology). Detection was carried out using enhanced chemiluminescence. Bands were quantified by densitometry using ImageQuant TL 8.1 image analysis software (GE Healthcare, PA, USA) and values were normalized to  $\beta$ -tubulin or AKT.

*Quantitative PCR.* Tissue RNA was extracted from freshly isolated tissues with the TRIzol Reagent (Invitrogen) and 0.5  $\mu$ g of RNA were reverse-transcribed using SuperScript<sup>TM</sup> III (Invitrogen, Carlsbad, CA) and Oligo (dT). RT-PCR was performed with 5 ng cDNA using primers described in **Supplemental Table 1**. The cycling conditions were 1 cycle at 95°C/10



min and 40 two-segment cycles of amplification (95°C/15 sec, 56°C/45 sec). Fluorescence was measured at 56°C/45 sec. The baseline adjustment method of the Bio-Rad CFX Manager™ version 3.0 software was used to determine the Ct in each reaction. A melting curve was used to verify the presence of one gene-specific peak and the absence of primer dimer. Results are presented as fold-change normalized to  $\beta$ -actin and wild-type expression using the  $2^{-\Delta\Delta Ct}$  method [22].

*Isolated Mesenteric Resistance Artery Preparation.* Second order mesenteric arteries were excised and segments were suspended between two cannulae in a pressure myograph system (Danish Myo Technology model 111P, Aarhus, Denmark). The bath was oxygenated in 95% O<sub>2</sub>/5% CO<sub>2</sub> Krebs physiological salt solution (119.0 mM NaCl, 25.0 mM NaHCO<sub>3</sub>, 4.6 mM KCL, 1.2 mM KH<sub>2</sub>PO<sub>4</sub>, 1.2 mM MgSO<sub>4</sub>, 1.8 mM CaCl<sub>2</sub>, 11.0 mM glucose) at pH 7.4 and 37°C. Under no-flow conditions, the vessel was pressurized from 10 mmHg to 60 mmHg in increments of 10 mmHg every 3 minutes. The vessel was then pressurized to 65 mmHg for 30 min for equilibration and kept at 65 mmHg for the remainder of the experiment. One vessel segment was used per experiment. Lumen diameter measurements were acquired and logged using the MyoVIEW 1.2P user interface. The control lumen diameter was measured as a mean over the last minute of the 30 min equilibration period. After being constricted with U46619, a thromboxane mimetic, the diameter was measured as a mean over the last 5 min of a 15 min period. Following U46619 constriction, vessel diameter responses to pinacidil (0.00 -10  $\mu$ M) were assessed and analyzed as percentage of relaxation from the maximum contraction.

*Metabolic assessment of human subjects.* All human studies were approved by the Vanderbilt Institutional Review Board, and subjects gave informed consent prior to enrollment into the study. Subjects with mild hypertension were recruited and washed out from anti-hypertensive

medications for at least 3 weeks prior to study, as described previously [23]. Subjects ingested calorie and sodium-controlled diets for 6 days, calculated for weight maintenance and to approximate the average regional sodium intake (200 mmol sodium/day, 100 mmol/day potassium, and 1000–1350 mg/day calcium.). Studies were conducted at 7AM after an overnight fast, and subjects remained supine for 1 hour before plasma was collected into tubes containing triphenylphosphine and frozen at -80 °C for measurement of EETs. Frequently sampled intravenous glucose tolerance tests (FSIVGTT) were then performed [24, 25], with an initial bolus of glucose (300 mg glucose/kg body weight) followed by an insulin bolus at t=20 minutes (0.02 units/kg body weight regular insulin; Actrapid, Novo Nordisk, Princeton, NJ). Plasma glucose was analyzed using the glucose oxidase method (YSI 2300 STAT Plus Glucose Analyzer, YSI Life Sciences; Yellow Springs, IL). Plasma insulin was measured by radioimmunoassay (Millipore, St. Charles, MO) [24, 25]. Free plasma EETs were quantified via high pressure liquid chromatography/tandem mass spectrometry as previously described [26]. The acute insulin response to glucose (AIRg), insulin sensitivity ( $S_i$ ), and disposition index were calculated from FSIVGTT data using the MINMOD Millennium software [27, 28].

*Statistical analysis and calculations.* Data are presented as mean  $\pm$  SEM in text and figures. Between-group comparisons were made using a two sample t-test for normally distributed data or Wilcoxon rank sum test for non-normally distributed data. Linear regression was performed to test the association between insulin sensitivity and plasma measurements in humans, and multivariate regression analysis was performed to adjust for potential confounding variables. Statistical analyses were performed with R (version 3.3)[29] and IBM<sup>®</sup> SPSS<sup>®</sup> for Windows (version 21, IBM<sup>®</sup> SPSS<sup>®</sup>, Chicago, IL), with a two-tailed  $p$ -value  $<0.05$  considered significant.

## RESULTS

**Streptozotocin-induced hyperglycaemia is augmented in *Cyp2c44*(-/-) mice.** Glucose tolerance tests performed on wild-type and *Cyp2c44*(-/-) mice revealed that glucose tolerance was significantly impaired in *Cyp2c44*(-/-) mice (**Figure 1A, 1B**;  $p=0.004$  for glucose area-under-the-curve, AUC). During studies to induce a type-1 diabetes model streptozotocin (STZ) treatment induced hyperglycaemia to a significantly greater extent in *Cyp2c44*(-/-) compared to WT mice (**Supplemental Figure 1**;  $30.3\pm 0.65$  vs.  $26.8\pm 0.58$  mmol/L average after STZ-treatment;  $p=0.023$  for genotype effect).

***Cyp2c44*-derived EETs contribute to peripheral and hepatic insulin sensitivity.** These differences in glucose suggested that endogenous *Cyp2c44*-derived EETs alter either insulin sensitivity or insulin secretion. To investigate the potential mechanisms, we performed hyperinsulinaemic-euglycaemic clamps during regular chow diet to assess insulin sensitivity in WT and *Cyp2c44*(-/-) mice. Blood glucose and insulin were similar in WT and *Cyp2c44*(-/-) mice after a 5-hour fast (**Table 1**). Although weight was slightly greater in *Cyp2c44*(-/-) mice during regular diet, both genotypes gained weight to a similar extent during high fat feeding. *Cyp2c44*(-/-) mice had less fat and more lean mass during regular chow diet, although there were no apparent differences after HF diet for 12 weeks.

During hyperinsulinaemic-euglycaemic clamp studies, similar insulin concentrations were achieved ( $313\pm 52$  vs.  $328\pm 81$  pmol/L in WT and *Cyp2c44*(-/-);  $p=0.91$ ). The glucose infusion rate needed to maintain euglycaemia near 6.4 mmol/L (**Figure 1C**) was significantly reduced in *Cyp2c44*(-/-) mice ( $2.24\pm 0.22$  vs.  $3.28\pm 0.14$  mmol/kg/min in *Cyp2c44*(-/-) and WT;  $p=0.003$ ), indicating impaired sensitivity to insulin (**Figure 1D**). Similarly, the rate of glucose disappearance ( $R_d$ ) was significantly reduced in *Cyp2c44*(-/-) compared to WT mice (**Figure 1E**;

$p=0.023$ ). As expected, HF diet impaired insulin sensitivity in WT mice (**Supplemental Figure 2A-C**). However, there was no further effect of *Cyp2c44* deficiency on insulin sensitivity during high fat diet.

Although endogenous glucose production (EndoR<sub>a</sub>) was similar under basal conditions ( $1.01\pm 0.01$  vs.  $1.2\pm 0.11$  mmol/kg/min in WT and *Cyp2c44*(-/-);  $p=0.12$ ), insulin infusion incompletely suppressed endogenous glucose production in *Cyp2c44*(-/-) mice (**Figure 1F**), indicating hepatic resistance to insulin. After acute insulin injection, hepatic AKT phosphorylation was significantly impaired in *Cyp2c44*(-/-) mice (**Figure 1G, 1H**). We conclude that endogenous *Cyp2c44*-derived EETs contribute to hepatic and peripheral insulin sensitivity *in vivo* in mice.

***Cyp2c44* disruption impairs muscle insulin sensitivity *in vivo* but not *in vitro*.** Tissue-specific glucose uptake at the termination of the hyperinsulinaemic-euglycaemic clamps was significantly reduced within *vastus lateralis*, gastrocnemius, and adipose tissues as measured by 2DG uptake (**Figures 2A, 2B, and 2C**). Potential mechanisms of this insulin resistance include impaired perfusion (reduced vascularity, diminished blood flow, or excess extracellular matrix) or impaired muscle sensitivity to insulin [30]. To control for tissue perfusion due to either altered blood flow or vascular density, we studied isolated soleus and *extensor digitorum longus* muscles from wild-type and *Cyp2c44*(-/-) mice and observed similar insulin-stimulated glucose uptake (assessed as [<sup>3</sup>H]2DG uptake) between the two genotypes (**Supplemental Figure 3A and 3B**). To determine whether skeletal muscle perfusion was impaired *in vivo*, we assessed skeletal muscle tissue perfusion using hindlimb ultrasound measurement after microbubble contrast injection, which demonstrated a non-significant decrease in cross-sectional area (**Supplemental Figure 3C**). Extracellular matrix accumulation and capillary density, assessed by anti-collagen

IV and anti-CD31 immunoreactivity were similar in WT and *Cyp2c44(-/-)* mice, and therefore do not explain the impaired insulin sensitivity (**Supplemental Figure 3D-F**).

**Glucose-stimulated insulin secretion is augmented in *Cyp2c44(-/-)* mice in isolated islets.** To assess glucose-stimulated insulin secretion *in vivo*, we performed hyperglycaemic clamps in WT and *Cyp2c44(-/-)* mice to acutely raise glucose to ~13.9 mmol/L (250 mg/dL, **Figure 3A**), and insulin was similar between genotypes (**Figure 3B**), except for a small but significantly increased value at the 15 minute time point (**Figure 3C**,  $73.1 \pm 4.6$  vs.  $92.5 \pm 7.8$  pmol/L;  $p=0.039$ ), and trend to increase at 100 min ( $p=0.063$ ). After 16 weeks of HF feeding, glucose-stimulated insulin concentrations were increased in both genotypes (**Supplemental Figure 4B**), but increased to a greater extent in *Cyp2c44(-/-)* mice (peak insulin  $150.8 \pm 20.3$  vs.  $269.7 \pm 46.4$  pmol/L in WT and *Cyp2c44(-/-)* mice;  $p=0.037$ ). The differences between *Cyp2c44(-/-)* and WT mice during HF diet remained after analyzing the insulin area-under-the-curve during the initial 20 minutes (**Supplemental Figure 4C**).

Isolated islets from *Cyp2c44(-/-)* mice demonstrated a significantly greater insulin response to glucose *in vitro* compared to WT islets (**Figure 4A**). Analysis of *Cyp2c44* mRNA from freshly isolated pancreatic islets confirmed the presence of this transcript in wild-type mice, but not in *Cyp2c44(-/-)* mice (**Figure 4B**). We also examined the expression of sEH (encoded by *Ephx2*) and long-chain acyl-CoA synthetase-4 (encoded by *Acsl4*) which reduce free intracellular EETs [31]. Expression of *Ephx2* (**Figure 4C**) and *Acsl4* mRNA (**Figure 4D**) were increased in *Cyp2c44(-/-)* islets. Immunofluorescence performed on pancreatic frozen sections confirmed the expression of anti-CYP2C reactive proteins which mainly localized to pancreatic beta cells (**Figure 4E**). In islets isolated after HF feeding, *Ephx2* mRNA expression also increased in both WT and *Cyp2c44(-/-)* islets, but to a greater extent in *Cyp2c44(-/-)* islets regardless of diet

**(Supplemental Figure 5B).**

***Cyp2c44* disruption impairs  $K_{ATP}$ -dependent relaxation in mesenteric resistance arteries.**

Because vascular endothelial dysfunction can impair tissue perfusion and insulin sensitivity, and EETs alter  $K_{ATP}$  activity, we assessed mesenteric resistance artery dilation to the  $K_{ATP}$  channel opener pinacidil. Mesenteric resistance artery diameter was similar between groups averaging  $128 \pm 14$   $\mu\text{m}$  in wild-type and  $133 \pm 10$   $\mu\text{m}$  in *Cyp2c44*(-/-) mice. Concentration-dependent mesenteric resistance artery relaxation to pinacidil was attenuated in *Cyp2c44*(-/-) compared to WT mice. **(Figure 5A)**. These data demonstrate that *Cyp2c44*(-/-) mice have an impaired mesenteric resistance artery dilation to  $K_{ATP}$  activation. To assess whether  $K_{ATP}$  sensitivity was altered in other tissues, we assessed the insulin response to the pancreatic islet  $K_{ATP}$  channel blocker glyburide *in vivo*, which demonstrated an impaired acute insulin response to glyburide in *Cyp2c44*(-/-) mice **(Figure 5B)**. To determine whether differences in  $K_{ATP}$  channel expression explained the impaired insulin sensitivity, we assessed protein expression of the  $K_{ATP}$  subunits Kir6.1 and Kir6.2 in skeletal muscle and observed no difference between the two genotypes **(Figure 5C and 5D)**. Similarly, skeletal muscle mRNA expression of Cyp2c isoforms demonstrated no change in *Cyp2c29*, *Cyp2c38* or *Cyp2c40* **(Supplemental Figure 6)**.

**Plasma EETs are associated with insulin resistance in humans.** We determined whether circulating levels of EETs correlate to insulin sensitivity in humans. Metabolic characteristics of 31 mildly hypertensive subjects were assessed after 3-weeks of anti-hypertensive medication washout **(Supplemental Table 2)** [23]. In univariate analyses, insulin sensitivity as assessed by FSIVGTT modeling ( $S_i$ ) did not correlate with age, gender, race, triglycerides, LDL cholesterol, systolic blood pressure or body mass index, but positively correlated with HDL cholesterol ( $p=0.004$ ). Insulin sensitivity positively correlated with plasma 8,9-EET, 11,12-EET, 14,15-EET

and total EET concentrations (**Figures 6A-D**). HDL cholesterol also associated with plasma 8,9-EET ( $p=0.035$ ), 11,12-EET ( $p=0.004$ ), and total EETs ( $p=0.016$ ), but not with 14,15-EET ( $p=0.061$ ). Plasma EETs remained associated with insulin sensitivity after multivariate analysis adjusting for HDL and body mass index (adjusted estimates presented in **Table 2**). Plasma EETs were not associated with the acute insulin response to glucose (AIRg) or with the disposition index.

## DISCUSSION

Genetic disruption of the EET-generating CYP450 epoxygenases results in hypertension, and inhibition of EET hydrolysis reduces blood pressure and improves glucose metabolism [3, 11]. The present study demonstrates that genetic disruption of *Cyp2c44* decreased peripheral and hepatic insulin sensitivity, increased isolated islet insulin secretion, and impaired vascular  $K_{ATP}$ -dependent vasodilation in mice. Furthermore, plasma EETs were strongly associated with insulin sensitivity in humans, supporting the conclusion that CYP2C-derived EETs increase insulin sensitivity, increase vascular reactivity, and reduce blood pressure.

Genetic *Cyp2c44* disruption decreased insulin sensitivity and impaired  $K_{ATP}$ -mediated vasodilation, but did not affect blood flow-independent insulin sensitivity in isolated muscle *ex vivo*, suggesting that altered vascular function accounts for diminished insulin sensitivity *in vivo*. Although decreased capillary density or increased matrix accumulation can also contribute to insulin resistance due to reduced tissue perfusion [32, 33], we observed no difference in vascular endothelial cell density or collagen deposition. Other studies suggest that the microvascular response to insulin is mediated in part via EETs. Increasing endogenous EETs via sEH inhibition increases insulin-mediated capillary blood volume and microvascular blood flow, whereas epoxygenase inhibition impaired this vasodilatory response [34]. Because *Cyp2c44*(-/-) mice are normotensive on a normal sodium diet [8, 10], vascular dysfunction in these mice is not due to hypertension-induced remodeling. Treatment with EET analogs or overexpression of CYP2C/2J genes decrease reactive oxygen species and production of pro-inflammatory cytokines, and this effect could also contribute to insulin sensitivity in *Cyp2c44*(-/-) mice [35, 36]. Impaired vasodilatory responsiveness is also associated with insulin resistance and hypertension [16, 37], and our studies implicate CYP2C-derived EETs as potential mediators.



We conclude that impaired vascular reactivity in *Cyp2c44(-/-)* mice likely contributes to impaired insulin sensitivity *in vivo*.

In the present study, all plasma EET isomers strongly associated with insulin sensitivity in humans. These studies were conducted under highly controlled conditions to minimize variability due to anti-hypertensive medications or dietary intake. We also observed a positive association between plasma EETs and HDL cholesterol, which has not been previously reported. EETs can increase HDL via peroxisome proliferator-activated receptor (PPAR)- $\alpha$  activation after CYP4A-dependent hydroxylation to form  $\omega$ -hydroxy-EETs [38]. Consistent with these findings, we previously identified that a reduced-function *CYP4A11* variant is associated with a reduction in plasma HDL in the Framingham Cohort [39]. Even after correction for HDL, plasma EETs were strongly associated with insulin sensitivity. It is possible that genetic polymorphisms which affect EET metabolism could modify diabetes risk in humans. We recently found that the Arg287Gln *EPHX2* variant, which is associated with decreased ability to hydrolyze EETs, is associated with increased insulin sensitivity [40]. The present study significantly expands on these findings by improved assessment of insulin sensitivity and significantly increased number of subjects. The *CYP2J-50T* polymorphism, which is associated with decreased EET production, has also been associated with an earlier age of onset and insulin resistance in a Chinese population with T2DM [41]. Further studies are needed to clarify these relationships and to investigate the potential effects of additional CYP polymorphisms.

Pancreatic islets possess the synthetic capacity to produce EETs *in vivo* [42], but the effect of CYP epoxygenase and EETs on insulin secretion is inconsistent across studies. We found that *Cyp2c44* disruption increased insulin secretion assessed during hyperglycaemic clamps *in vivo* in high fat-fed mice. Similarly, we found that *Cyp2c44* disruption increased

insulin secretion in isolated islets *in vitro*, consistent with the hypothesis that free endogenous EETs decrease insulin secretion. In a prior study using isolated rat islets, 5,6-EET stimulated insulin secretion, whereas other isomers stimulated glucagon secretion [43]. CYP2C enzymes including Cyp2c44 generate little if any 5,6-EET, however, and predominantly generate 8,9-, 11,2-, and 14,15-EET [3]. Other investigators have not observed significant EET synthesis or an effect of exogenous EETs on insulin secretion in isolated rat islets [44]. The effect of EETs on insulin secretion may differ for free versus membrane EETs. Long-chain acyl-CoA synthetase-4 (Acsl4) acetylates endogenous EETs, which are reincorporated into cell membrane glycerophospholipids, decreasing the free intracellular pool. Klett *et al* recently reported that Acsl4 knockdown increased free EETs, decreased membrane EETs, and impaired insulin secretion in an insulinoma cell line. [31]. In our studies, islet *Ephx2* and *Acsl4* mRNA expression were increased in *Cyp2c44(-/-)* mice without compensatory changes in Cyp2c isoforms, suggesting a decrease in intracellular EETs. Other studies have not observed any compensatory change in Cyp2c isoforms in *Cyp2c44(-/-)* mice [8]. An increase in islet *Ephx2* mRNA expression occurred after HF diet, consistent with the effect of HF diet in liver and adipose tissues [45, 46]. The finding that insulin secretion was increased in mice lacking Cyp2c44 supports the conclusion that endogenous free intracellular EETs decrease insulin secretion within isolated islets.

The effect of EETs on ATP-sensitive potassium ( $K_{ATP}$ ) channels may account for altered vascular function, insulin sensitivity, and insulin secretion in *Cyp2c44(-/-)* mice.  $K_{ATP}$  channels are the drug target for sulfonylureas and are composed of four pore-forming inwardly rectifying potassium channels (either  $K_{ir}6.1$  or  $K_{ir}6.2$ ) and four sulfonylurea receptor (either SUR1 or SUR2A) regulatory subunits.  $K_{ATP}$  channels are primarily composed of  $K_{ir}6.1/SUR2A$  subunits

in vascular smooth muscle and  $K_{ir}6.2/SUR1$  within pancreatic islets [47]. In the present study, Cyp2c44 disruption impaired vasodilation during  $K_{ATP}$  channel opener pinacidil administration, suggesting that endogenous Cyp2c44-derived EETs are essential for maximal  $K_{ATP}$ -dependent vasodilatory response. EETs activate  $K_{ATP}$  channels in vascular smooth muscle cells [48], and decreasing endogenous EETs via vascular soluble epoxide hydrolase overexpression impairs the vascular response to pinacidil [49]. Our studies are the first to demonstrate that genetic deletion of the principal Cyp2c isoform, Cyp2c44, modulates vascular  $K_{ATP}$  responsiveness.

Our findings demonstrate that CYP2C-derived EETs affect insulin sensitivity and vascular reactivity, and suggest that this system is a potential link between hypertension and T2DM. Further studies are needed to determine whether interventions to increase EETs have a net favorable effect on glucose metabolism in humans, and promising EET agonists and sEH inhibitors are in development.

**Acknowledgements.** We thank Tasneem Ansari and Carlo Malabanan (Vanderbilt MMPC) for their excellent technical expertise during clamp studies, and Shuozei Wei for performing analysis of plasma EETs.

**Funding.** This work was supported by grants from the NIH (DK095761, DK081662, DK038226, HL060906), the Veteran Affairs (I01 BX002025-01) and the Vanderbilt Mouse Metabolic Phenotyping Center (DK59637). Clinical studies were supported by UL1 RR024975 and UL1 TR000445 from NCATS/NIH (Vanderbilt Institute for Clinical and Translational Research). Hormone assays and islet stimulation studies were performed by the Vanderbilt Diabetes Research and Training Center Hormone Assay Core Lab and Islet Procurement and Analysis Core Lab (DK20593).

**Contribution Statement.** MHG, BWD, LL, CFK, LK, DHW, MC, CFC, AP, and JML designed experiments. MHG, BWD, LL, LK, MC, JD, PL, JDI, AP and JML collected data. MHG, DHW, JHC, JDI, CY, AP, and JML analyzed and interpreted data. All authors critically reviewed the manuscript and approved the final version.

**Duality of Interest.** No potential conflicts of interest relevant to this article were reported.

## BIBLIOGRAPHY & REFERENCES CITED

1. Kahn SE, Hull RL, Utzschneider KM (2006) Mechanisms linking obesity to insulin resistance and type 2 diabetes. *Nature* 444: 840-846
2. Reaven G (2012) Insulin resistance and coronary heart disease in nondiabetic individuals. *Arterioscler Thromb Vasc Biol* 32: 1754-1759
3. Imig JD (2012) Epoxides and soluble epoxide hydrolase in cardiovascular physiology. *Physiol Rev* 92: 101-130
4. Roman RJ, Maier KG, Sun CW, Harder DR, Alonso-Galicia M (2000) Renal and cardiovascular actions of 20-hydroxyeicosatetraenoic acid and epoxyeicosatrienoic acids. *Clin Exp Pharmacol Physiol* 27: 855-865
5. Spector AA, Fang X, Snyder GD, Weintraub NL (2004) Epoxyeicosatrienoic acids (EETs): metabolism and biochemical function. *Prog Lipid Res* 43: 55-90
6. Campbell WB, Fleming I (2010) Epoxyeicosatrienoic acids and endothelium-dependent responses. *Pflugers Arch* 459: 881-895
7. Capdevila J, Wang W (2013) Role of cytochrome P450 epoxygenase in regulating renal membrane transport and hypertension. *Curr Opin Nephrol Hypertens* 22: 163-169
8. Sun P, Antoun J, Lin DH, et al. (2012) Cyp2c44 epoxygenase is essential for preventing the renal sodium absorption during increasing dietary potassium intake. *Hypertension* 59: 339-347
9. DeLozier TC, Tsao CC, Coulter SJ, et al. (2004) CYP2C44, a new murine CYP2C that metabolizes arachidonic acid to unique stereospecific products. *J Pharmacol Exp Ther* 310: 845-854
10. Capdevila JH, Pidkovka N, Mei S, et al. (2014) The Cyp2c44 epoxygenase regulates epithelial sodium channel activity and the blood pressure responses to increased dietary salt. *J Biol Chem* 289: 4377-4386
11. Sodhi K, Inoue K, Gotlinger KH, et al. (2009) Epoxyeicosatrienoic acid agonist rescues the metabolic syndrome phenotype of HO-2-null mice. *J Pharmacol Exp Ther* 331: 906-916
12. Theken KN, Deng Y, Schuck RN, et al. (2012) Enalapril reverses high-fat diet-induced alterations in cytochrome P450-mediated eicosanoid metabolism. *Am J Physiol Endocrinol Metab* 302: E500-509
13. Luo P, Chang HH, Zhou Y, et al. (2010) Inhibition or deletion of soluble epoxide hydrolase prevents hyperglycemia, promotes insulin secretion, and reduces islet apoptosis. *J Pharmacol Exp Ther* 334: 430-438
14. Luria A, Bettaieb A, Xi Y, et al. (2011) Soluble epoxide hydrolase deficiency alters pancreatic islet size and improves glucose homeostasis in a model of insulin resistance. *Proc Natl Acad Sci U S A* 108: 9038-9043
15. Iyer A, Kauter K, Alam MA, et al. (2012) Pharmacological inhibition of soluble epoxide hydrolase ameliorates diet-induced metabolic syndrome in rats. *Experimental diabetes research* 2012: 758614
16. Mather KJ, Steinberg HO, Baron AD (2013) Insulin resistance in the vasculature. *J Clin Invest* 123: 1003-1004
17. Zanchi A, Maillard M, Jornayvaz FR, et al. (2010) Effects of the peroxisome proliferator-activated receptor (PPAR)-gamma agonist pioglitazone on renal and hormonal responses to salt in diabetic and hypertensive individuals. *Diabetologia* 53: 1568-1575
18. Imig JD, Zhao X, Zaharis CZ, et al. (2005) An orally active epoxide hydrolase inhibitor lowers blood pressure and provides renal protection in salt-sensitive hypertension. *Hypertension* 46: 975-981
19. Luther JM, Luo P, Kreger MT, et al. (2011) Aldosterone decreases glucose-stimulated insulin secretion in vivo in mice and in murine islets. *Diabetologia* 54: 2152-2163
20. Remedi MS, Agapova SE, Vyas AK, Hruz PW, Nichols CG (2011) Acute sulfonyleurea therapy at disease onset can cause permanent remission of KATP-induced diabetes. *Diabetes* 60: 2515-2522

21. Williams CA, Shih MF, Taberner PV (1999) Sustained improvement in glucose homeostasis in lean and obese mice following chronic administration of the beta 3 agonist SR 58611A. *Br J Pharmacol* 128: 1586-1592
22. Livak KJ, Schmittgen TD (2001) Analysis of relative gene expression data using real-time quantitative PCR and the 2(-Delta Delta C(T)) Method. *Methods* 25: 402-408
23. Gilbert K, Nian H, Yu C, Luther JM, Brown NJ (2013) Fenofibrate lowers blood pressure in salt-sensitive but not salt-resistant hypertension. *J Hypertens* 31: 820-829
24. Hill KD, Eckhauser AW, Marney A, Brown NJ (2009) Phosphodiesterase 5 inhibition improves beta-cell function in metabolic syndrome. *Diabetes Care* 32: 857-859
25. Ayers K, Byrne LM, DeMatteo A, Brown NJ (2012) Differential effects of nebivolol and metoprolol on insulin sensitivity and plasminogen activator inhibitor in the metabolic syndrome. *Hypertension* 59: 893-898
26. Karara A, Wei S, Spady D, Swift L, Capdevila JH, Falck JR (1992) Arachidonic acid epoxygenase: structural characterization and quantification of epoxyeicosatrienoates in plasma. *Biochem Biophys Res Commun* 182: 1320-1325
27. Bergman RN, Finegood DT, Ader M (1985) Assessment of insulin sensitivity in vivo. *Endocr Rev* 6: 45-86
28. Boston RC, Stefanovski D, Moate PJ, Sumner AE, Watanabe RM, Bergman RN (2003) MINMOD Millennium: a computer program to calculate glucose effectiveness and insulin sensitivity from the frequently sampled intravenous glucose tolerance test. *Diabetes Technol Ther* 5: 1003-1015
29. R Core Team (2014) R: A Language and Environment for Statistical Computing. R Foundation for Statistical Computing, Vienna, Austria, URL: <https://www.R-project.org/>.
30. Wasserman DH (2009) Four grams of glucose. *Am J Physiol Endocrinol Metab* 296: E11-21
31. Klett EL, Chen S, Edin ML, et al. (2013) Diminished acyl-CoA synthetase isoform 4 activity in INS 832/13 cells reduces cellular epoxyeicosatrienoic acid levels and results in impaired glucose-stimulated insulin secretion. *J Biol Chem* 288: 21618-21629
32. Kang L, Lantier L, Kennedy A, et al. (2013) Hyaluronan accumulates with high-fat feeding and contributes to insulin resistance. *Diabetes* 62: 1888-1896
33. Kang L, Ayala JE, Lee-Young RS, et al. (2011) Diet-induced muscle insulin resistance is associated with extracellular matrix remodeling and interaction with integrin alpha2beta1 in mice. *Diabetes* 60: 416-426
34. Shim CY, Kim S, Chadderdon S, et al. (2014) Epoxyeicosatrienoic acids mediate insulin-mediated augmentation in skeletal muscle perfusion and blood volume. *Am J Physiol Endocrinol Metab* 307: E1097-1104
35. Chen W, Yang S, Ping W, Fu X, Xu Q, Wang J (2015) CYP2J2 and EETs protect against lung ischemia/reperfusion injury via anti-inflammatory effects in vivo and in vitro. *Cell Physiol Biochem* 35: 2043-2054
36. Liu W, Wang B, Ding H, Wang DW, Zeng H (2014) A potential therapeutic effect of CYP2C8 overexpression on anti-TNF-alpha activity. *Int J Mol Med* 34: 725-732
37. Laakso M, Edelman SV, Brechtel G, Baron AD (1990) Decreased effect of insulin to stimulate skeletal muscle blood flow in obese man. A novel mechanism for insulin resistance. *J Clin Invest* 85: 1844-1852
38. Cowart LA, Wei S, Hsu MH, et al. (2002) The CYP4A isoforms hydroxylate epoxyeicosatrienoic acids to form high affinity peroxisome proliferator-activated receptor ligands. *J Biol Chem* 277: 35105-35112
39. White CC, Feng Q, Cupples LA, et al. (2013) CYP4A11 variant is associated with high-density lipoprotein cholesterol in women. *Pharmacogenomics J* 13: 44-51
40. Ramirez CE, Shuey MM, Milne GL, et al. (2014) Arg287Gln variant of EPHX2 and epoxyeicosatrienoic acids are associated with insulin sensitivity in humans. *Prostaglandins Other Lipid Mediat* 113-115: 38-44

41. Wang CP, Hung WC, Yu TH, et al. (2010) Genetic variation in the G-50T polymorphism of the cytochrome P450 epoxygenase CYP2J2 gene and the risk of younger onset type 2 diabetes among Chinese population: potential interaction with body mass index and family history. *Exp Clin Endocrinol Diabetes* 118: 346-352
42. Zeldin DC, Foley J, Boyle JE, et al. (1997) Predominant expression of an arachidonate epoxygenase in islets of Langerhans cells in human and rat pancreas. *Endocrinology* 138: 1338-1346
43. Falck JR, Manna S, Moltz J, Chacos N, Capdevila J (1983) Epoxyeicosatrienoic acids stimulate glucagon and insulin release from isolated rat pancreatic islets. *Biochem Biophys Res Commun* 114: 743-749
44. Turk J, Wolf BA, Comens PG, Colca J, Jakschik B, McDaniel ML (1985) Arachidonic acid metabolism in isolated pancreatic islets. IV. Negative ion-mass spectrometric quantitation of monooxygenase product synthesis by liver and islets. *Biochim Biophys Acta* 835: 1-17
45. Liu Y, Dang H, Li D, Pang W, Hammock BD, Zhu Y (2012) Inhibition of soluble epoxide hydrolase attenuates high-fat-diet-induced hepatic steatosis by reduced systemic inflammatory status in mice. *PLoS One* 7: e39165
46. De Taeye BM, Morisseau C, Coyle J, et al. (2010) Expression and regulation of soluble epoxide hydrolase in adipose tissue. *Obesity* 18: 489-498
47. Flagg TP, Enkvetchakul D, Koster JC, Nichols CG (2010) Muscle KATP channels: recent insights to energy sensing and myoprotection. *Physiol Rev* 90: 799-829
48. Lu T, Ye D, Wang X, et al. (2006) Cardiac and vascular KATP channels in rats are activated by endogenous epoxyeicosatrienoic acids through different mechanisms. *J Physiol* 575: 627-644
49. Yadav VR, Hong KL, Zeldin DC, Nayeem MA (2016) Vascular endothelial over-expression of soluble epoxide hydrolase (Tie2-sEH) enhances adenosine A1 receptor-dependent contraction in mouse mesenteric arteries: role of ATP-sensitive K<sup>+</sup> channels. *Mol Cell Biochem* 422: 197-206

## FIGURE LEGENDS

**Figure 1. Cyp2c44 disruption impairs glucose tolerance and insulin sensitivity.** Glucose tolerance was impaired in *Cyp2c44*(-/-) mice after glucose administration (A), and as quantified as glucose area-under-the-curve (AUC, B). Wild-type (WT) and *Cyp2c44*(-/-) mice were studied during hyperinsulinaemic-euglycaemic clamps on a regular chow diet. Glucose was similarly maintained in all groups during the hyperinsulinaemic studies (C). The glucose infusion rate (GIR, D) and rate of glucose disappearance ( $R_d$ , E) were significantly reduced in *Cyp2c44*(-/-) mice. Endogenous rate of glucose appearance ( $EndoR_a$ ) was incompletely suppressed in *Cyp2c44*(-/-) mice at the end of the clamp (F). Liver tissues were collected 10-15 minutes after i.p. insulin (10 mU) or saline injection, and Western blots for pAKT and AKT (G) showed significantly impaired phosphorylation of AKT after insulin treatment in *Cyp2c44*(-/-) mice (H). \* $p < 0.05$ , \*\* $p < 0.01$ , \*\*\* $p < 0.001$  between genotype.

**Figure 2. Cyp2c44 disruption impairs peripheral tissue glucose uptake during hyperinsulinaemic-euglycaemic clamps.** Tissue glucose uptake was decreased in *Cyp2c44*(-/-) mice as assessed by  $^{14}C$ -2-deoxyglucose uptake during hyperinsulinaemic-euglycaemic clamps in *vastus lateralis* (A), gastrocnemius (B), and adipose (C) tissues. \* $p < 0.05$ , \*\* $p < 0.01$  between genotype.

**Figure 3. Glucose-stimulated insulin secretion during hyperglycaemic clamps is unchanged in *Cyp2c44*(-/-) mice during regular chow feeding.** During hyperglycaemic clamps to assess insulin secretion, glucose increased to 200-250mg/dL (11.1-13.3 mmol/L, A) by dextrose infusion, and plasma insulin was assessed (B). Insulin during the initial 20 minutes of the study increased to a similar extent in *Cyp2c44*(-/-) mice (C).

**Figure 4. Cyp2c44 disruption increases insulin secretion in isolated islets.** In isolated islets cultured in normal (5.6 mM) or high glucose (16.7 mM) for 60 minutes, glucose-stimulated insulin secretion was increased in *Cyp2c44(-/-)* islets (A). *Cyp2c44* mRNA expression was detected in isolated wild-type (WT) but not *Cyp2c44(-/-)* islets (B). sEH (Ephx2, C) and *Acs14* mRNA expression (D) demonstrated increased expression in *Cyp2c44(-/-)* mice. Immunostaining of pancreatic sections for CYP2C (green) and Insulin (red) demonstrated localization to insulin-positive cells (E). \* $p < 0.05$ , \*\*\* $p < 0.001$ .

**Figure 5. Cyp2c44 disruption impairs K<sub>ATP</sub>-mediated vascular relaxation.** Mesenteric resistance artery endothelium-independent vasodilation in response to the ATP-sensitive potassium channel opener pinacidil was impaired in *Cyp2c44(-/-)* mice compared to wild-type control vessels (A). After administration of the K<sub>ATP</sub>-channel blocker glyburide, the plasma insulin response was diminished in *Cyp2c44(-/-)* compared to wild-type mice (B). Western blots for the K<sub>ATP</sub>-channel subunits Kir6.1 (C) and Kir6.2 (D) subunits in skeletal muscle demonstrated similar expression. \* $p < 0.05$ , \*\*\* $p < 0.001$  between genotype.

**Figure 6. Plasma EETs correlate with insulin sensitivity in humans.** Insulin sensitivity assessed during frequently sampled intravenous glucose tolerance tests correlates with plasma EET isomers (A, 8,9-; B, 11,12-; C, 14,15-; D, total) in mildly hypertensive human subjects. Pearson correlation coefficient ( $r$ ) and  $p$ -value are presented for each. Each data point (blue circle) represents measurements from an individual subject. Linear regression lines (solid) are displayed with 95% confidence intervals (dashed lines).



**Table 1. Metabolic characteristics of wild-type (WT) and *Cyp2c44*(-/-) mice on high-fat diet**

	WT	<i>Cyp2c44</i> (-/-)	WT + HF	<i>Cyp2c44</i> (-/-) + HF
Weight (g)	29.0±0.68	33.2±0.98 <sup>***</sup>	37.6±0.92 <sup>†††</sup>	35.4±1.09
Fasting glucose (mg/dL)	110.8±6.6	104.3±5.3	125.3±4.3	123.5±4.8 <sup>†</sup>
Fasting insulin (mg/dL)	1.17±0.14	1.67±0.21	1.79±0.24 <sup>†</sup>	2.91±0.52 <sup>†</sup>
Peri-gonadal fat weight (g)	0.51±0.05	0.51±0.06	2.01±0.12 <sup>†††</sup>	1.77±0.17 <sup>†††</sup>
Visceral fat weight (g)	0.261±0.081	0.298±0.132	0.600±0.081 <sup>†††</sup>	0.607±0.133 <sup>†††</sup>
Body composition Fat (g)	3.35±0.25	2.32±0.19 <sup>**</sup>	13.14±2.74 <sup>††</sup>	12.74±0.08 <sup>†††</sup>
Body composition Muscle (g)	19.95±0.49	22.02±0.72 <sup>*</sup>	21.69±1.32	18.19±0.89 <sup>†</sup>
Body composition Free Fluid (g)	0.24±0.044	0.41±0.082	0.69±0.025 <sup>††</sup>	0.66±0.034

Data are mean±SEM

HF, high fat-feeding.

For comparisons between genotype, within diet, <sup>\*</sup> $p<0.05$ , <sup>\*\*</sup> $p<0.01$ , <sup>\*\*\*</sup> $p<0.001$

For comparisons between diet, within genotype, <sup>†</sup> $p<0.05$ , <sup>††</sup> $p<0.01$ , <sup>†††</sup> $p<0.001$

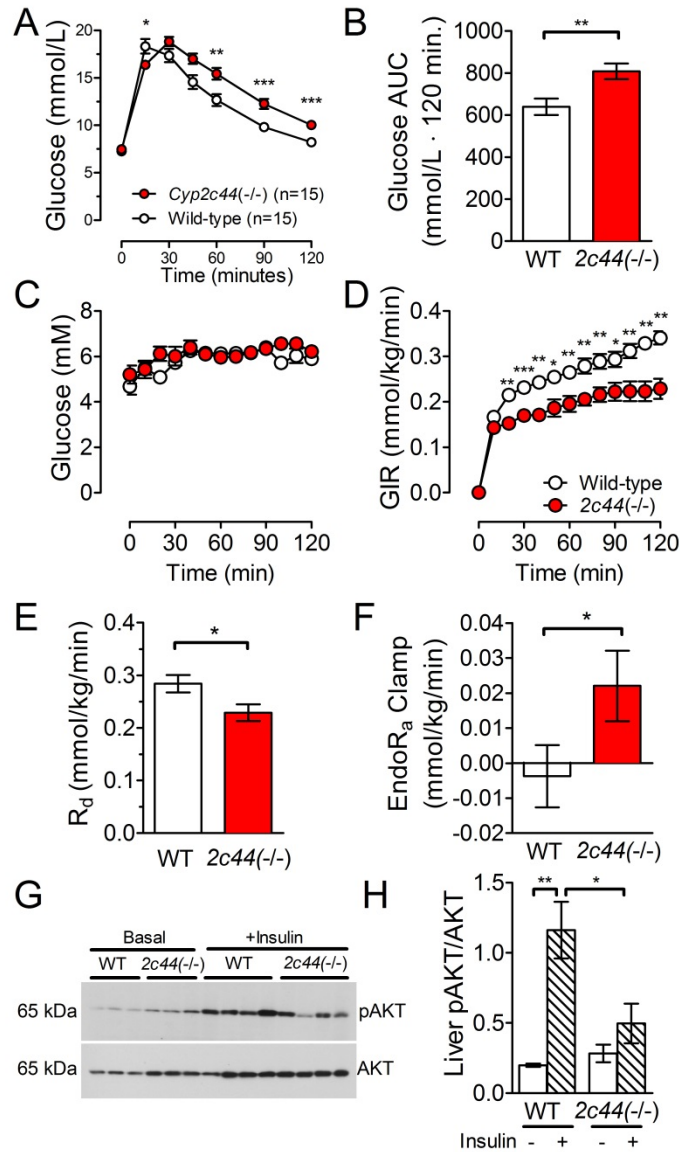
$n\geq 12$  in each group, except body composition data available in only 3 wild-type + HF and 2 *Cyp2c44*(-/-) + HF.

**Table 2. Multivariate-adjusted analysis of insulin sensitivity and plasma EETs in humans**

	<b>Standardized</b>	<b>β-coefficient</b>	<b>p-value</b>
	<b>coefficient</b>	<b>(95% CI)</b>	
8,9-EET	0.78	0.0053 (0.0037,0.0069)	<10 <sup>-6</sup>
11,12-EET	0.55	0.0094 (0.0026, 0.015)	0.007
14,15-EET	0.25	0.0052 (-0.0033, 0.011)	0.27
Total EETs	0.68	0.0016 (0.0016, 0.0041)	<10 <sup>-4</sup>

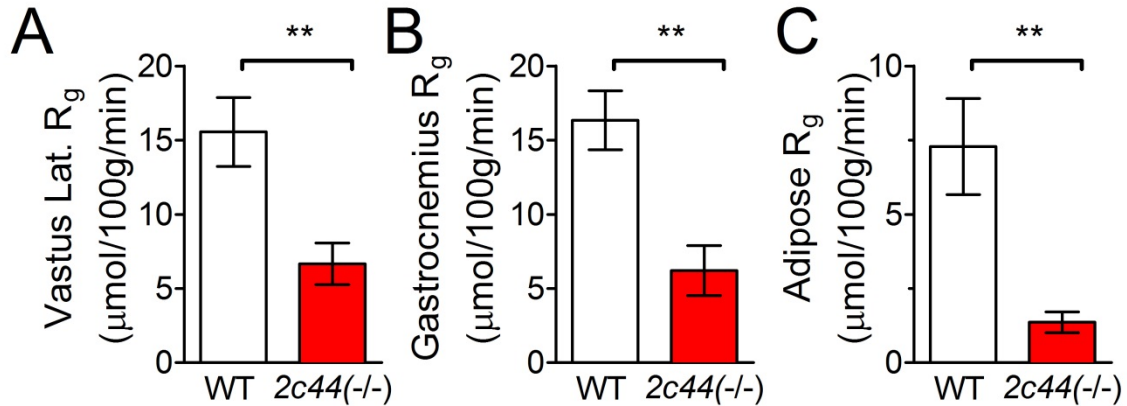
Multivariate analysis of insulin sensitivity index assessed during frequently sampled intravenous glucose tolerance tests in 31 mildly hypertensive subjects, adjusted for body mass index and HDL cholesterol.

**Figure 1**



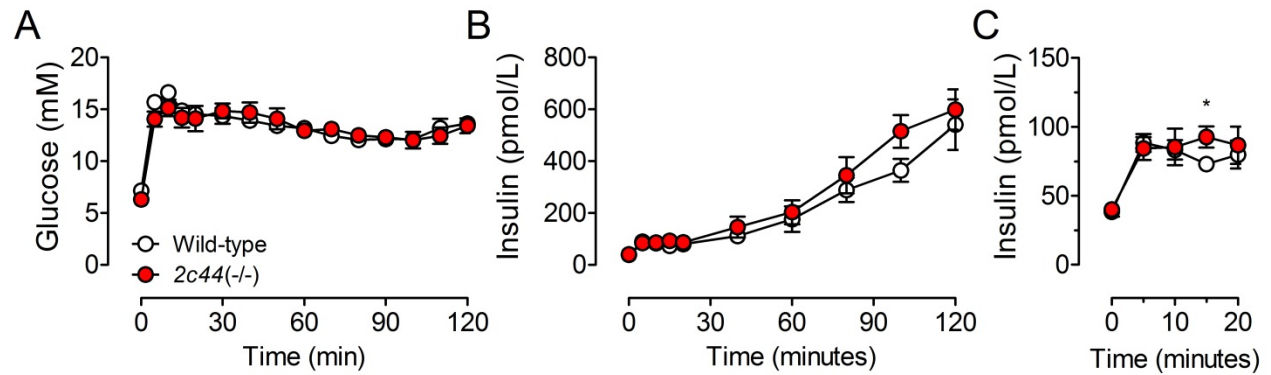
**Figure 1. *Cyp2c44* disruption impairs glucose tolerance and insulin sensitivity.** Glucose tolerance was impaired in *Cyp2c44*<sup>-/-</sup> mice after glucose administration (A), and as quantified as glucose area-under-the-curve (AUC, B). Wild-type (WT) and *Cyp2c44*<sup>-/-</sup> mice were studied during hyperinsulinaemic-euglycaemic clamps on a regular chow diet. Glucose was similarly maintained in all groups during the hyperinsulinaemic studies (C). The glucose infusion rate (GIR, D) and rate of glucose disappearance ( $R_d$ , E) were significantly reduced in *Cyp2c44*<sup>-/-</sup> mice. Endogenous rate of glucose appearance (Endo $R_a$ ) was incompletely suppressed in *Cyp2c44*<sup>-/-</sup> mice at the end of the clamp (F). Liver tissues were collected 10-15 minutes after i.p. insulin (10 mU) or saline injection, and Western blots for pAKT and AKT (G) showed significantly impaired phosphorylation of AKT after insulin treatment in *Cyp2c44*<sup>-/-</sup> mice (H). \* $p < 0.05$ , \*\* $p < 0.01$ , \*\*\* $p < 0.001$  between genotype.

Figure 2



**Figure 2. Cyp2c44 disruption impairs peripheral tissue glucose uptake during hyperinsulinaemic-euglycaemic clamps.** Tissue glucose uptake was decreased in *Cyp2c44*(-/-) mice as assessed by <sup>14</sup>C-2-deoxyglucose uptake during hyperinsulinaemic-euglycaemic clamps in *vastus lateralis* (A), *gastrocnemius* (B), and *adipose* (C) tissues. \**p*<0.05, \*\**p*<0.01 between genotype.

**Figure 3**



**Figure 3. Glucose-stimulated insulin secretion during hyperglycaemic clamps is unchanged in *Cyp2c44*<sup>-/-</sup> mice during regular chow feeding.** During hyperglycaemic clamps to assess insulin secretion, glucose increased to 200-250mg/dL (11.1-13.3 mmol/L, **A**) by dextrose infusion, and plasma insulin was assessed (**B**). Insulin during the initial 20 minutes of the study increased to a similar extent in *Cyp2c44*<sup>-/-</sup> mice (**C**).

**Figure 4**

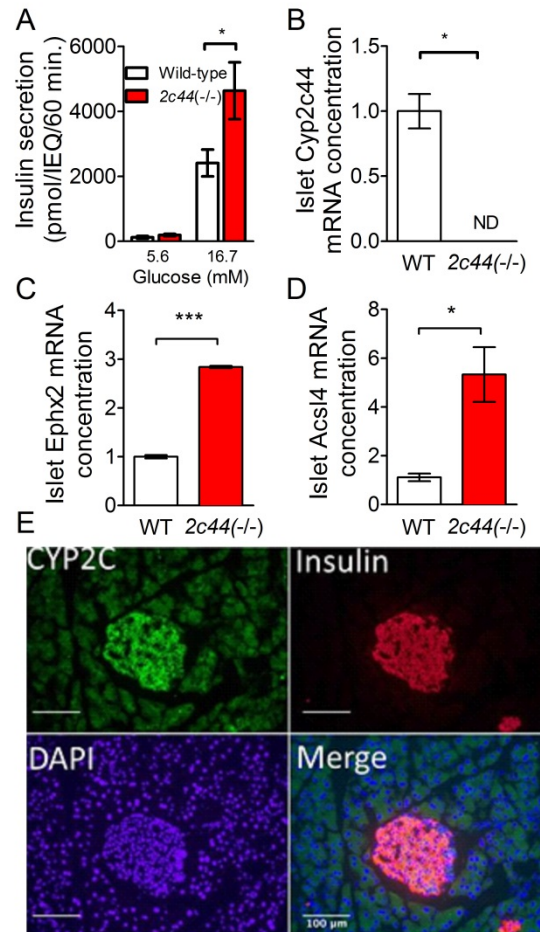


**Figure 4. Cyp2c44 disruption increases insulin secretion in isolated islets.** In isolated islets cultured in normal (5.6 mM) or high glucose (16.7 mM) for 60 minutes, glucose-stimulated insulin secretion was increased in *Cyp2c44*(-/-) islets (**A**). *Cyp2c44* mRNA expression was detected in isolated wild-type (WT) but not *Cyp2c44*(-/-) islets (**B**). sEH (Ephx2, **C**) and *Acsl4* mRNA expression (**D**) demonstrated increased expression in *Cyp2c44*(-/-) mice. Immunostaining of pancreatic sections for CYP2C (green) and Insulin (red) demonstrated localization to insulin-positive cells (**E**). \* $p < 0.05$ , \*\*\* $p < 0.001$ .

**Figure 5**

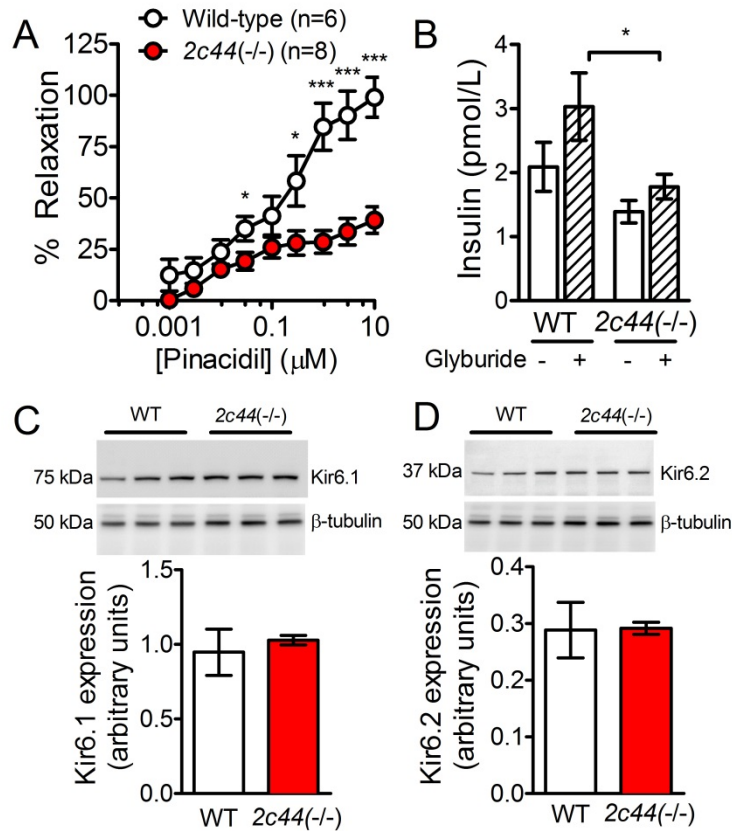


**Figure 5. *Cyp2c44* disruption impairs  $K_{ATP}$ -mediated vascular relaxation.** Mesenteric resistance artery endothelium-independent vasodilation in response to the ATP-sensitive potassium channel opener pinacidil was impaired in *Cyp2c44(-/-)* mice compared to wild-type control vessels (A). After administration of the  $K_{ATP}$ -channel blocker glyburide, the plasma insulin response was diminished in *Cyp2c44(-/-)* compared to wild-type mice (B). Western blots for the  $K_{ATP}$ -channel subunits Kir6.1 (C) and Kir6.2 (D) subunits in skeletal muscle demonstrated similar expression. \* $p < 0.05$ , \*\*\* $p < 0.001$  between genotype.

**Figure 6**

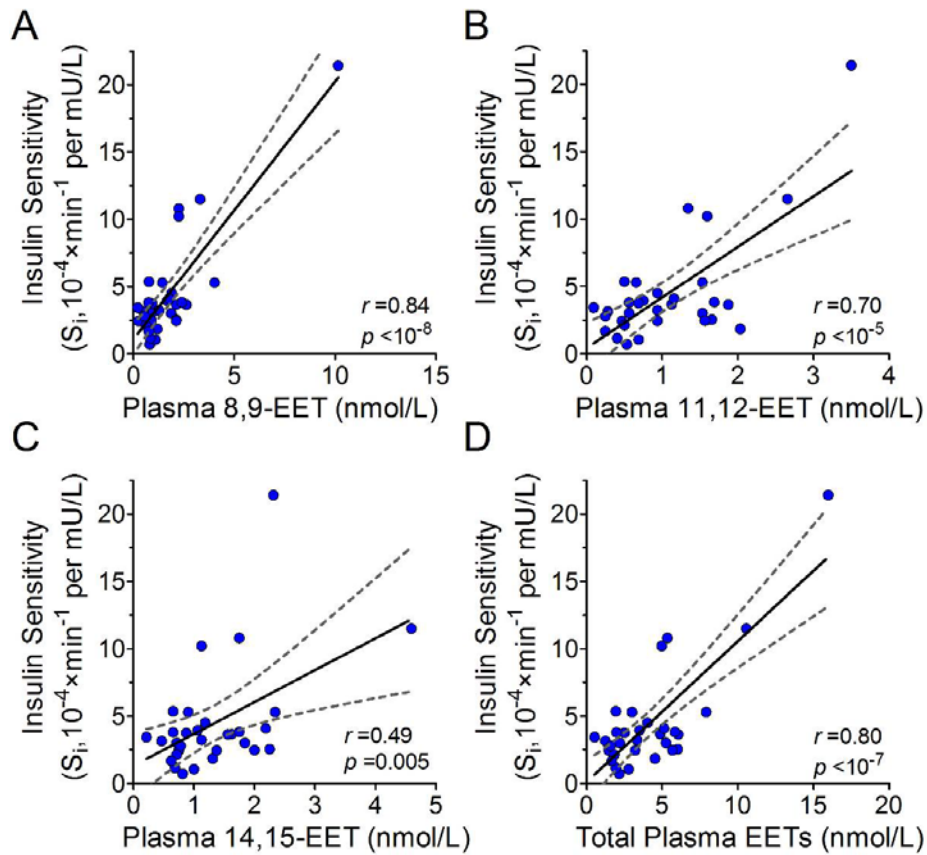


**Figure 6. Plasma EETs correlate with insulin sensitivity in humans.** Insulin sensitivity assessed during frequently sampled intravenous glucose tolerance tests correlates with plasma EET isomers (**A**, 8,9-; **B**, 11,12-; **C**, 14,15-; **D**, total) in mildly hypertensive human subjects. Pearson correlation coefficient ( $r$ ) and  $p$ -value are presented for each. Each data point (blue circle) represents measurements from an individual subject. Linear regression lines (solid) are displayed with 95% confidence intervals (dashed lines).



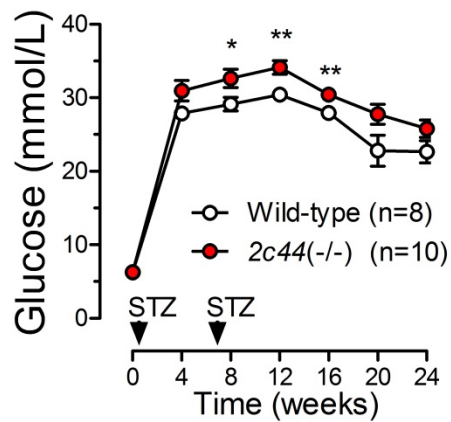
## **SUPPLEMENTARY DATA**

### **Cytochrome P450 Epoxygenase-Derived Epoxyeicosatrienoic Acids Contribute to Insulin Sensitivity in Mice and in Humans**

M.H. Gangadhariah<sup>1</sup>, B.W. Dieckmann<sup>1</sup>, L. Lantier<sup>2</sup>, L. Kang<sup>2</sup>, D.H. Wasserman<sup>2</sup>, M. Chiusa<sup>1</sup>, C.F. Caskey<sup>3</sup>, J. Dickerson<sup>4</sup>, P. Luo<sup>5</sup>, J.H. Capdevila<sup>1</sup>, J.D. Imig<sup>6</sup>, C. Yu<sup>7</sup>, A. Pozzi<sup>1,9</sup>, J.M. Luther<sup>1,8</sup>

**Running title: CYP2C-derived EETs and Insulin sensitivity**

## Supplemental Figure 1



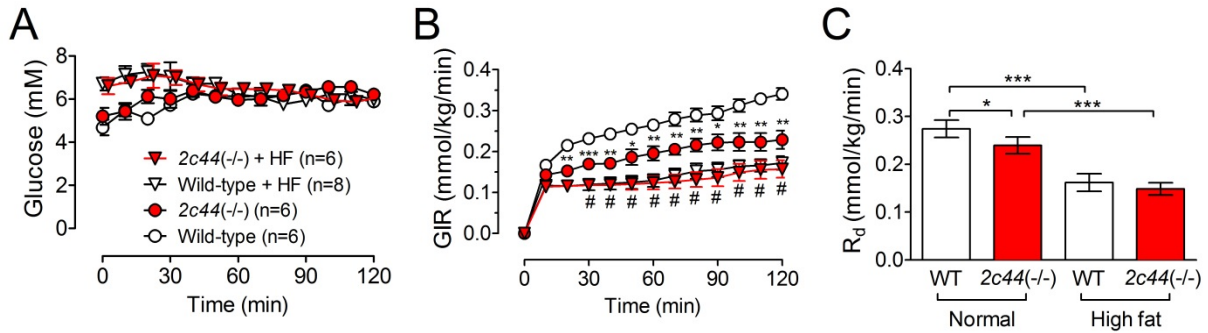
**Cyp2c44 disruption impairs glucose tolerance and fasting glucose after streptozotocin treatment.** A, Fasting blood glucose was assessed in wild-type and *Cyp2c44*(-/-) mice every 2 weeks after streptozotocin (STZ) administration at weeks 0 and 7.

\* $p < 0.05$ , \*\* $p < 0.01$ , \*\*\* $p < 0.001$  between genotypes for each time point.

### *Streptozotocin Treatment.*

Eight week-old 129SvJ wild-type and *Cyp2c44*(-/-) mice were injected with streptozotocin (50 mg/kg i.p., made freshly in 0.1M sodium citrate buffer, pH 4.5) or vehicle once a day for 5 consecutive days. Blood glucose levels were measured 1 week after the last streptozotocin injection and mice with fasting blood glucose levels  $>350$  mg/dl were considered diabetic. To maintain chronic hyperglycaemia, mice were injected with streptozotocin 7 weeks after induction of hyperglycaemia according to Animal Models of Diabetic Complications Consortium recommendations [<http://www.diacomp.org/shared/protocols.aspx>]. Blood glucose was measured mice using Bayer Breeze® 2 (Bayer HealthCare LLC, Whippany, NJ) after a 5 hour fast.

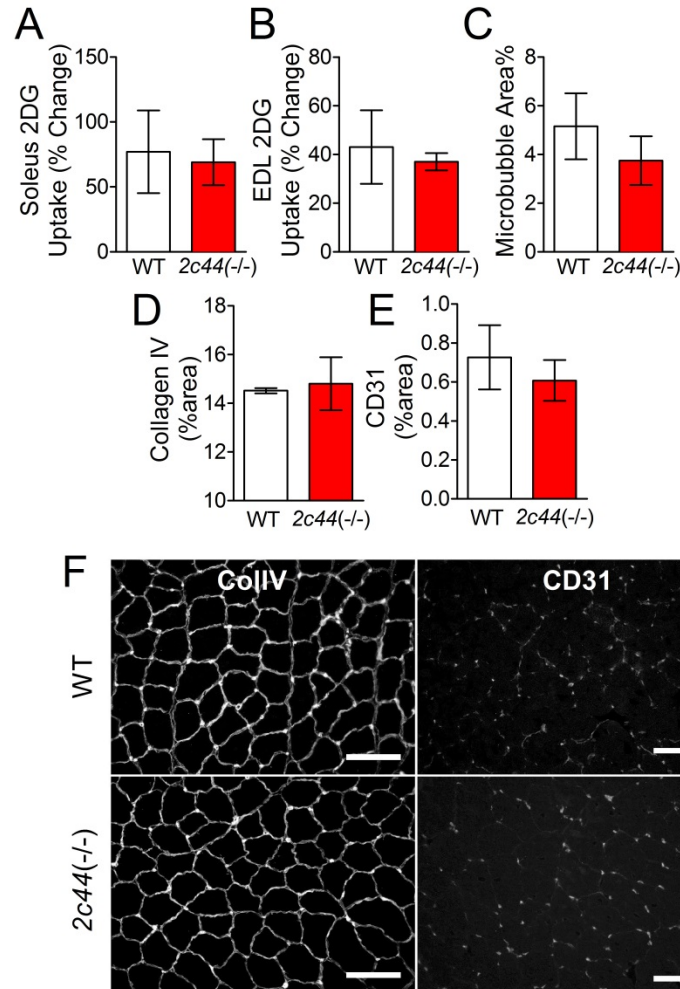
## Supplemental Figure 2



**Cyp2c44 disruption impairs *in vivo* insulin sensitivity during hyperinsulinemic-euglycemic clamps.** Wild-type (WT) and *Cyp2c44*(-/-) mice were kept on either regular chow or high fat diet (HF) for 16 weeks prior hyperinsulinemic-euglycemic clamps. Glucose was similarly maintained in all groups between 100-120 mg/dL during the hyperinsulinemic studies (**A**). The glucose infusion rate (GIR, **B**) and rate of glucose disappearance ( $R_d$ ) (**C**) were significantly reduced in *Cyp2c44*(-/-) mice and in both high fat-fed groups. Endogenous rate of glucose appearance ( $EndoR_a$ ) in wild-type (WT) and *Cyp2c44*(-/-) mice was incompletely suppressed in *Cyp2c44*(-/-) mice.

\* $p < 0.05$ , \*\* $p < 0.01$ , \*\*\* $p < 0.001$  (between genotype in B). # $p < 0.05$  between diet for both WT and *Cyp2c44*(-/-) mice.

### Supplemental Figure 3.



**Ex vivo tissue glucose uptake and extracellular matrix assessment.** Muscle tissues were freshly isolated from age-matched wild-type (WT) and *Cyp2c44*<sup>-/-</sup> mice to assess insulin-stimulated 2-deoxyglucose (2DG) uptake *ex vivo* (n=8 in each group). Insulin-stimulated 2DG uptake was similar in *soleus* (A) and *extensor digitorum longus* (EDL) (B). Tissue perfusion as measured in mice using microbubble contrast, showed no significant differences between wild-type and *Cyp2c44*<sup>-/-</sup> mice (C). Extracellular matrix accumulation as measured by collagen IV area (D, F) and capillary density as measured by CD31 positive-area (E, F) per microscopic field was similar between genotype (scale bar = 100  $\mu$ m).

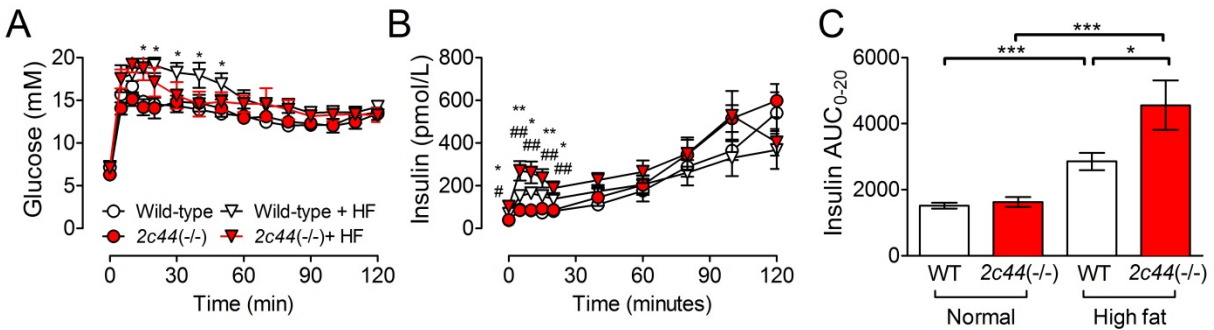
*Isolated muscle glucose uptake measurements.* We assessed isolated muscle 2[<sup>3</sup>H]deoxyglucose ([<sup>3</sup>H]2DG) uptake in 12-16-week old wild-type and *Cyp2c44*<sup>-/-</sup> mice on normal chow diet. In brief, *soleus* and *extensor digitorum longus* (EDL) muscles were excised and treated with or

without insulin 10 mU/mL for 30 minutes, and [<sup>3</sup>H]2DG was measured 10 minutes after adding cold 2DG (1 mmol/L, [<sup>3</sup>H]2DG (0.25 μCi/mL), and D-[<sup>14</sup>C]mannitol (0.16 μCi/mL) [20, 21].

*Microbubble methods.* Tissue perfusion was assessed in mice under isoflurane anesthesia using contrast-enhanced doppler ultrasound after retro-orbital bolus of 100 μL perflutren microbubble contrast diluted 1:5 in saline (Lantheus Medical Imaging, N. Billerica, MA, USA). Cross-sectional imaging of the *vastus lateralis* muscle was performed at baseline and immediately after microbubble injection (Visualsonics RMV 704; SonoSite Inc., Toronto, Ontario, Canada). Tissue flow was quantified as cross-sectional area after adjustment for baseline signal in ImageJ.

*Histology and Immunohistochemistry.* Unfixed, frozen *vastus lateralis* muscle sections (10 μm) were stained with either rat anti-CD31 (BD Biosciences, 1:1,000) or rabbit anti-collagen IV (Chemicon, 1:1,000) and imaged after incubation with donkey Cy3-conjugated species-specific secondary antibody (Jackson ImmunoResearch, 1:500). Digitally captured images (20x objective) were quantified for percent immune-positive area per field using ImageJ software version 1.51a (NIH, Bethesda, MD) [22].

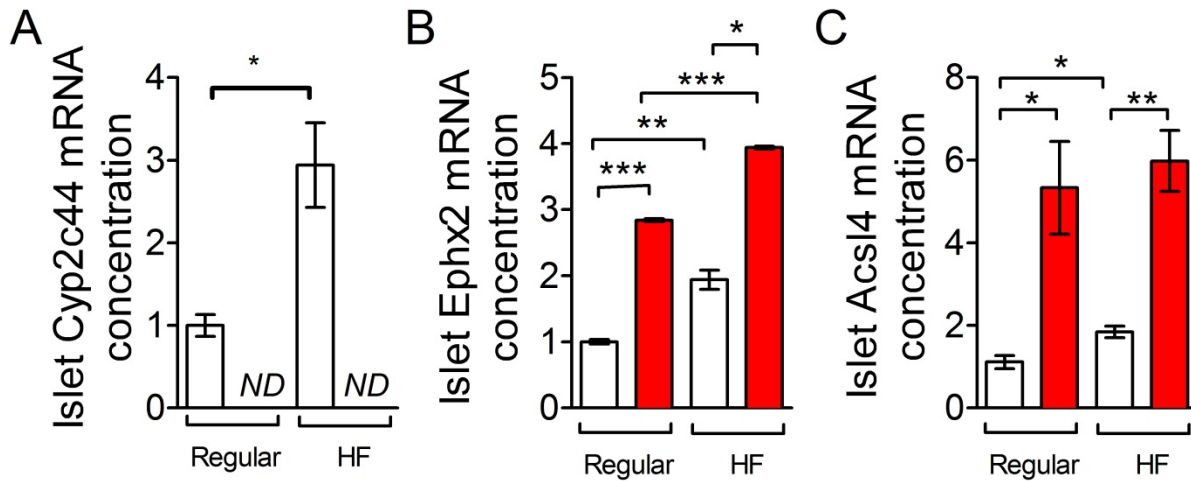
## Supplemental Figure 4



**Glucose-stimulated insulin secretion during hyperglycemic clamps is augmented in *Cyp2c44*(-/-) mice during high fat feeding.** After wild-type (WT) or *Cyp2c44*(-/-) mice were fed either normal or high fat diets for 16 weeks, hyperglycemic clamps were performed to assess insulin secretion (A-C). Plasma glucose was acutely increased to ~250mg/dL (A) by infusion of dextrose, and plasma insulin was assessed (B). The area-under-the-curve insulin during the initial 20 minutes (C) increased during high fat-feeding to a greater extent in *Cyp2c44*(-/-) mice.

\* $p < 0.05$ , \*\* $p < 0.01$ , \*\*\* $p < 0.001$  (between diet in B). #  $p < 0.05$ , ## $p < 0.01$ , (between genotype in HF groups in B).

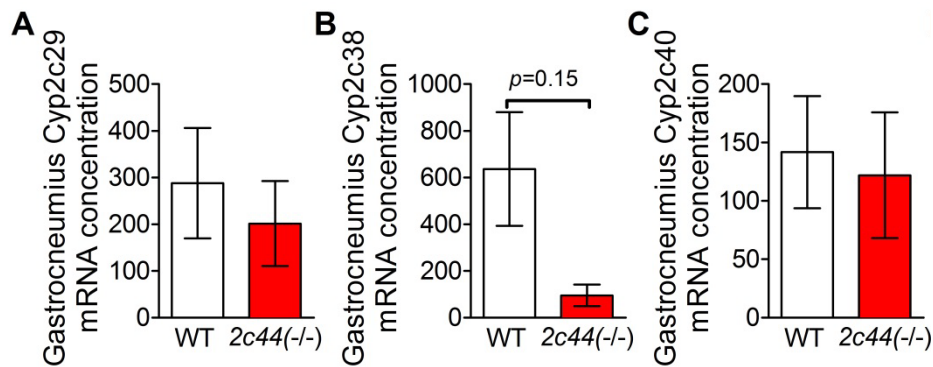
## Supplemental Figure 5



**Cyp2c gene expression in isolated islets.** Quantitative PCR for expression of Cyp2c44 mRNA detected expression in isolated WT but not *Cyp2c44*(-/-) islets, and increased expression during high fat (HF)-feeding (A). Quantitative PCR for sEH (Ephx2) demonstrated increased expression during high-fat feeding and in *Cyp2c44*(-/-) mice (B). Islet Acsl4 expression was increased in *Cyp2c44*(-/-) islets and in WT islets after HF (C).

\* $p < 0.05$ , \*\* $p < 0.01$ , \*\*\* $p < 0.001$ .

## Supplemental Figure 6



**Cyp2c gene expression in skeletal muscle.** Quantitative PCR for expression of Cyp2c isoforms detected unchanged expression of Cyp2c29 in *Cyp2c44(-/-)* gastrocnemius (A). Expression of Cyp2c38 was lower, although not statistically different in the *Cyp2c44(-/-)* mice. (B), Expression of Cyp2c40 was unchanged (C).

\* $p < 0.05$ , \*\* $p < 0.01$ .



**Supplemental Table 1. PCR Primer sequences**

<b>Gene</b>	<b>Direction</b>	<b>Sequence</b>
$\beta$ -actin	Forward	5'-CAGGATGCAGAAGGAGATCAC-3'
	Reverse	5'-TGTC AAGAAAGGGTGT AACGC-3'
Cyp2c29	Forward	5'-GCTATGGATCTGGTCGTGTTC-3'
	Reverse	5'-TTCCTTCACTGCTTCATACCC-3'
Cyp2c38	Forward	5'-ATGCTACAAACCCTCGTGAC-3'
	Reverse	5'-TGAATCATGGCATCAGTATAGGG-3'
Cyp2c40	Forward	5'-TGCTTGTCCTGTCATTGTGG-3'
	Reverse	5'-ACCAATGCCCTTTCCTGTAG-3'
Cyp2c44	Forward	5'-CAGGCACAGAGACAACCAG-3'
	Reverse	5'-AGACAGAAACGGGAACACAG-3'
Cyp2j5	Forward	5'-TTGGGTGGAACAGAGACAAC-3'
	Reverse	5'-GTGCAGTCAAATTGGTCAGG-3'
Cyp4a10	Forward	5'-TGAGCTGAAGGTGATTGTGG-3'
	Reverse	5'-TGAACAGAGGATGAGAGGACT-3'
Cyp4a12	Forward	5'-TCCTTCTCGATTTGCACCAG-3'
	Reverse	5'-ACAGAAAGACAGAATGGCAGG-3'
Cyp4a14	Forward	5'-TTCTGCCCTCATTTCTGTAGC-3'
	Reverse	5'-TGATGTCCATTGTCCCAAGAG-3'
Ephx2	Forward	5'-TGTA AAGGGTTGGGACGAAAG-3'
	Reverse	5'-TGGCTAAATCTTGGAGGTCAC-3'
Acsl4	Forward	5'-GGGTAGAAGGATCTTGGGTTG-3'
	Reverse	5'-CTCCTGTGCAAATGGAAATCAG-3'

**Supplemental Table 2. Subject characteristics**

	<b>Mean±SE or n (%)</b>
Age (years)	43.3±2.0
Sex (Male:Female)	15 (48%) : 16 (52%)
Race (White: Black)	20 (65%) : 11 (35%)
Weight (kg)	88.3±3.9
Body mass index (kg/m <sup>2</sup> )	29.6±1.0
Systolic blood pressure (mmHg)	136.4±2.3
Diastolic blood pressure (mmHg)	81.9±1.8
Heart rate (bpm)	63.7±2.1
HDL Cholesterol (mmol/L)	1.24±0.07
LDL Cholesterol (mmol/L)	2.70±0.15
Triglycerides (mmol/L)	0.87±0.06
<b>Free plasma epoxyeicosatrienoic acid (EET, nmol/L)</b>	
8,9-EET	1.76±0.32
11,12-EET	1.07±0.14
14,15-EET	1.33±0.15
Total EETs	4.16±0.56
<b>Frequently sampled intravenous glucose tolerance test results</b>	
Fasting glucose (mmol/L)	5.03±0.09
Fasting insulin (mU/L)	13.3±3.9
Acute insulin response to glucose (mU•L <sup>-1</sup> •min)	477.7±68.3
Insulin sensitivity index (S <sub>i</sub> , 10 <sup>-4</sup> /min per mU/L)	4.47±0.73
Disposition index (U)	1543.6±190.8

HDL, high density lipoprotein; LDL, low density lipoprotein